Available online at www.sciencedirect.com
SCIENCE DIRECT®
International Journal of Heat and Mass Transfer 47 (2004) 4697–4712
International Journal of HEAT and MASS TRANSFER
www.elsevier.com/locate/ijhmt

Effect of heat transfer on stability and transition characteristics of boundary-layers

Serkan Özgen

Department of Aerospace Engineering, Middle East Technical University, 06531 Ankara, Turkey

Received 5 September 2003; received in revised form 28 May 2004
Available online 20 July 2004

Abstract

Stability and transition problems of two dimensional boundary-layers with heated walls have been studied numerically using the linear stability theory. Incompressible stability equations have been modified to account for the variation of temperature dependent fluid properties across the layer. The equations obtained have been solved with an efficient shoot-search technique. Low speed flows of air and water have been analyzed with a wide range of heat transfer rates. In addition to the mean velocity profile characteristics, variable viscosity and density terms in the stability equations also have considerable influence on the results of the stability and transition analysis.

PACS: 47.20.−k; 44.20.+b; 47.15.Fe
Keywords: Flow instabilities; Boundary-layer heat transfer; Laminar to turbulent transition

1. Introduction

The stability and transition problems of boundary-layer flows with heat transfer effects are interesting for a number of practical applications. Among these, the flow of air over heated aircraft wings (to prevent icing) or fluid flow through heat exchangers may be considered. For such cases, the first effect of heating (or cooling) is to modify the velocity boundary-layer profile due to variable fluid properties. In terms of the stability problem, the governing equations are modified to account for the variable property effects. For these reasons, it is beyond any doubt that the stability and transition properties of such flows should be different from isothermal flows. Investigation of the extent of this deviation is an interesting problem both practically and academically.

The boundary-layer stability problem under the effect of heat transfer has been studied by several scientists in the past. Among these, Wazzan et al. [1] have reported a numerical study on the stability of water flow over heated or cooled flat plates. In that study, the Orr–Sommerfeld equation has been modified to account for variable viscosity in the boundary-layer and has been integrated starting from the freestream towards the wall. It has been found out that heat transfer has considerable influence on stability properties. The results show that heating stabilizes the flow and this is largely due to velocity profile shape. It is also mentioned that viscosity gradient in the layer has a strong destabilizing effect.

The work of Hauptmann [2] is significant in the sense that an algebraic expression has been obtained that relates the heat transfer rate to the point of instability following a perturbation method. The results are valid

E-mail address: sozgen@ae.metu.edu.tr.

0017-9310/$ - see front matter © 2004 Elsevier Ltd. All rights reserved.
doi:10.1016/j.ijheatmasstransfer.2004.05.026

Nomenclature

A	disturbance amplitude
$\vec{A}^i$	characteristic vector of the eigenvalue problem
a^i_j	element of the characteristic vector
C^*_p	specific heat at constant pressure
c	$c_r + \mathrm{i}c_i$, complex wave velocity
c_r	phase velocity
c_i	amplification factor
c_g	$\partial\omega_r/\partial\alpha$, group velocity
F	ρU, dimensionless streamfunction
H	δ^*/θ, boundary-layer shape factor
k^*	heat conduction coefficient
L^*	$\sqrt{v^*_e x^*/U^*_e}$, Blasius length scale
n	$\ln(A/A_0)$ amplitude ratio
P	mean pressure
p	instantaneous pressure
$\hat{p}$	perturbation pressure
$\bar{p}$	amplitude function of the perturbation pressure
R	$U^*_e L^*/v^*_e$, Reynolds number based on Blasius length scale
R_{x^*}	$U^*_e x^*/v^*_e$, Reynolds number based on streamwise distance, x^*
R_{δ^*}	$U^*_e \delta^*/v^*_e$, Reynolds number based on boundary-layer displacement thickness, δ^*
S^*_1	110 K, constant in Sutherland's viscosity formula
T	mean temperature
T_r	$T^*/273.15$ K, dimensionless temperature in fluid property relations for water
t	time
U, V	mean velocities in streamwise and normal directions
u, v	instantaneous velocities in streamwise and normal directions
$\hat{u}, \hat{v}$	perturbation velocities in streamwise and normal directions
$\bar{u}, \bar{v}$	amplitude functions of the perturbation velocity components
X_i	unknown functions in the system of equations
x, y	Cartesian coordinates
$\vec{X}^i$	solution vector of the eigenvalue problem

Greek symbols

α	wave number
β	Falkner–Skan parameter
δ^*	boundary-layer displacement thickness
θ	boundary-layer momentum thickness
λ_i	characteristic value of the eigenvalue problem
μ	dynamic viscosity
v	μ/ρ, kinematic viscosity
ρ	density
σ	$\mu^* C^*_p/k^*$, Prandtl number
σ_{xx}, σ_{yy}	normal stress components
τ_{xy}, τ_{yx}	shear stress components
Ω	ω_r/R dimensionless frequency of the propagating wave
ω	$\alpha(c_r + \mathrm{i}c_i)$, complex frequency

Subscripts

cr	critical condition
iso	isothermal condition
e	boundary-layer edge condition
0	property evaluated at the first neutrally stable point
tr	transition condition
w	wall condition

Superscripts

*	dimensional quantity
$'$	y-derivative
$\wedge$	perturbation quantity
–	amplitude of the perturbation quantity

for low to moderate heat transfer rates and show that water flows are stabilized by heating, whereas air flows are destabilized.

On the other hand, Herwig and Schäfer [3] have solved an extended version of the Orr–Sommerfeld equation including the effects of temperature and pressure dependent fluid properties. These effects have been treated by using Taylor series expansions with respect to temperature and pressure. It has been observed that decreasing the viscosity in the near wall region stabilizes the flow, while a uniformly decreased viscosity has a destabilizing effect.

In a more recent study, Schäfer et al. [4] have investigated the effect of heat transfer on the stability of boundary-layers by solving an extended version of the Orr–Sommerfeld equation also introduced in Ref. [3]. Heat transfer rates were assumed to be small and the leading order effects were found to be the temperature and pressure dependencies of viscosity and density. The asymptotic solutions obtained hold for all Newtonian fluids with Prandtl number remaining as a parameter.

The study of Lee [5] as mentioned in [6], treats the effects of heat transfer on the stability and transition

properties of a water boundary-layer on a flat plate. To this end, a modified version of the Orr–Sommerfeld equation has been solved which accounts for temperature dependent viscosity. Low to moderate heat transfer rates have been considered. Both the critical Reynolds number and the transition Reynolds number increase with increasing wall temperature.

On the experimental side, the work of Liepmann and Fila [7] is important. Liepmann and Fila have related the transition Reynolds number of an air flow to the wall temperature. They have found that the transition occurs earlier when the plate is heated and they have held the deviation of the velocity profiles from the Blasius profile responsible for this.

In the present study, the stability and transition issues of low speed boundary-layers under the influence of heat transfer are addressed. For this purpose, a fourth order differential equation system is solved in which the effects of temperature dependent viscosity, density and Prandtl number are accounted for. Here, due to low speed flow, pressure dependencies of fluid properties are assumed to be much smaller than temperature dependencies and hence are neglected (see also [3,4]). The equations solved in this study are the extended versions of the stability equations for incompressible flow proposed by Mack [8] and are solved by an efficient shoot-search technique described in detail by Özgen et al. [9]. The equations and the solution method are not restricted to low heat transfer rates but they are limited to the validity ranges of the empirical relations used for fluid properties (density, viscosity and the Prandtl number). In this context, the study complements and extends the previous work on the topic. Transition problem is also addressed, which was left relatively untouched by previous investigators. In addition to these, comparisons with previous experimental data are done as well.

First, the basic equations and their solution methods will be introduced in Sections 2 and 3, respectively. In Section 4, the results will be presented and discussed. Finally, the conclusions gathered from the study will be summarized in Section 5.

2. Basic equations

2.1. Stability equations

The system of equations governing the stability problem are derived starting from the equations of motion for two dimensional compressible flow written in Cartesian coordinates [10]:

$$\frac{\partial u^*}{\partial t^*}+u^*\frac{\partial u^*}{\partial x^*}+v^*\frac{\partial u^*}{\partial y^*}=-\frac{1}{\rho^*}\frac{\partial p^*}{\partial x^*}+\frac{1}{\rho^*}\frac{\partial \sigma^*_{xx}}{\partial x^*}+\frac{1}{\rho^*}\frac{\partial \tau^*_{xy}}{\partial y^*}, \tag{1}$$

$$\frac{\partial v^*}{\partial t^*}+u^*\frac{\partial v^*}{\partial x^*}+v^*\frac{\partial v^*}{\partial y^*}=-\frac{1}{\rho^*}\frac{\partial p^*}{\partial y^*}+\frac{1}{\rho^*}\frac{\partial \tau^*_{yx}}{\partial x^*}+\frac{1}{\rho^*}\frac{\partial \sigma^*_{yy}}{\partial y^*}, \tag{2}$$

$$\frac{\partial(\rho^* u^*)}{\partial x^*}+\frac{\partial(\rho^* v^*)}{\partial y^*}=0. \tag{3}$$

Eqs. (1) and (2) are the x- and y-momentum equations, respectively, while Eq. (3) is the continuity equation. Asterisks (*) denote dimensional properties. The stress components are given as:

$$\sigma^*_{xx}=2\mu^*\frac{\partial u^*}{\partial x^*},\quad \tau^*_{xy}=\tau^*_{yx}=\mu^*\left(\frac{\partial u^*}{\partial y^*}+\frac{\partial v^*}{\partial x^*}\right),$$
$$\sigma^*_{yy}=2\mu^*\frac{\partial v^*}{\partial y^*}. \tag{4}$$

Flow is separated into steady mean and unsteady perturbation components:

$$u^*(x^*,y^*,t^*)=U^*(x^*,y^*)+\hat{u}^*(x^*,y^*,t^*), \tag{5}$$
$$v^*(x^*,y^*,t^*)=V^*(x^*,y^*)+\hat{v}^*(x^*,y^*,t^*), \tag{6}$$
$$p^*(x^*,y^*,t^*)=P^*(x^*,y^*)+\hat{p}^*(x^*,y^*,t^*). \tag{7}$$

Perturbations are taken as two dimensional because according to Squire theorem two dimensional disturbances lead to instability earlier than three dimensional ones. It has been shown by Yih [11] that the theory holds for variable property flows as well as constant property flows.

These terms are inserted into Eqs. (1)–(3) and several simplifying assumptions are made:

- According to linear theory, disturbances are small so quadratic terms can be neglected ($\hat{u}^*\partial\hat{u}^*/\partial x^*$, etc.).
- Mean flow satisfies the equations of motion and is steady.
- Parallel flow assumption is used, i.e. $U^*=U^*(y^*)$ only and $V^*=0$.
- Similarly, temperature is a function of y^* only, $T^*=T^*(y^*)$.
- Fluid properties are functions of temperature (hence y^*) only, $\mu^*=\mu^*(T^*)$, $\rho^*=\rho^*(T^*)$ and $\sigma=\sigma(T^*)$.

Resulting equations for the perturbations are made dimensionless by choosing a suitable reference for each variable. Velocities are normalized by U^*_e, lengths by L^* (the choice for this parameter will explained below), temperatures by T^*_e, densities by ρ^*_e, pressures by $\rho^*_e U^{*2}_e$ and viscosities by μ^*_e. Subscript e denotes boundary-layer edge (or freestream) properties. Using the temporal stability formulation, the disturbances can be expressed in a Fourier series:

$$(\hat{u},\hat{v},\hat{p})=(\bar{u},\bar{v},\bar{p})e^{i\alpha(x-ct)}, \tag{8}$$

where α is the wave number, $c=c_r+ic_i$ is the complex wave velocity and the quantities with a bar are the disturbance amplitudes for their respective flow variables.

While the real part of the complex wave velocity is the phase velocity, the imaginary part is the amplification factor determining whether a disturbance is stable ($c_i<0$), neutrally stable ($c_i=0$) or unstable ($c_i>0$).

Following the steps mentioned above, the following set of equations for the perturbation quantities are obtained:

$$\mathrm{i}(\alpha U-\omega)\bar{u}+\bar{v}U' = -\frac{1}{\rho}\mathrm{i}\alpha\bar{p}+\frac{\mu}{\rho R}(\bar{u}''-2\alpha^2\bar{u}+\mathrm{i}\alpha\bar{v}')+\frac{\mu'}{\rho R}(\bar{u}'+\mathrm{i}\alpha\bar{v}), \tag{9}$$

$$\mathrm{i}(\alpha U-\omega)\bar{v} = -\frac{1}{\rho}\bar{p}'+\frac{\mu}{\rho R}(2\bar{v}''-\alpha^2\bar{v}+\mathrm{i}\alpha\bar{u}')+\frac{2\mu'}{\rho R}\bar{v}', \tag{10}$$

$$\rho(\mathrm{i}\alpha\bar{u}+\bar{v}')+\rho'\bar{v}=0. \tag{11}$$

In the above, primes ($'$) denote differentiation with respect to y and $\omega=\alpha c$ is the complex frequency. Reynolds number is defined as $R=\rho_e^*U_e^*L^*/\mu_e^*$. These equations are subject to the wall and freestream boundary conditions:

$$\bar{u}(0)=\bar{v}(0)=0, \tag{12}$$

$$\bar{u},\bar{v}\to 0 \quad \text{as } y\to\infty. \tag{13}$$

Isothermal stability equations can be obtained by substituting $\mu=1$, $\rho=1$, $\mu'=0$ and $\rho'=0$ to Eqs. (9)–(11).

As the boundary conditions are homogeneous, the above system constitutes an eigenvalue problem and there is a non-trivial solution only for certain combinations of α, ω and R. The dispersion relation can be expressed as:

$$\omega=\Psi(\alpha,R). \tag{14}$$

Eqs. (9)–(11) constitute a fourth order system for $\bar{u}$, $\bar{v}$, $\bar{p}$ and $\bar{u}'$. These equations can be combined to yield a single fourth order equation which is in fact an extended version of the Orr–Sommerfeld equation solved by Wazzan [1]. In this study, the current equations has been retained because they require only the first derivative of viscosity with respect to temperature and they are more general in the sense that they can be extended to treat high speed flows as well.

The above equations can be reduced to a system of first order equations by defining four new variables as follows:

$$X_1=\alpha\bar{u}, \tag{15}$$

$$X_2=\alpha\bar{u}', \tag{16}$$

$$X_3=\bar{v}, \tag{17}$$

$$X_4=\bar{p}. \tag{18}$$

With these definitions, Eqs. (9)–(11) can be rewritten as follows:

$$X_1'=X_2, \tag{19}$$

$$X_2'=\left[\alpha^2+\mathrm{i}\frac{\rho R}{\mu}(\alpha U-\omega)\right]X_1-\frac{\mu'}{\mu}X_2+\left[\alpha\frac{\rho R}{\mu}U'+\mathrm{i}\alpha^2\left(\frac{\rho'}{\rho}-\frac{\mu'}{\mu}\right)\right]X_3+\mathrm{i}\alpha^2\frac{R}{\mu}X_4, \tag{20}$$

$$X_3'=-\mathrm{i}X_1-\frac{\rho'}{\rho}X_3, \tag{21}$$

$$X_4'=\left[2\mathrm{i}\frac{\rho'}{\rho}\frac{\mu}{R}-2\mathrm{i}\frac{\mu'}{R}\right]X_1-\mathrm{i}\frac{\mu}{R}X_2+\left[-\mathrm{i}\rho(\alpha U-\omega)-2\frac{\rho''}{\rho}\frac{\mu}{R}+4\frac{\rho'^2}{\rho^2}\frac{\mu}{R}-\alpha^2\frac{\mu}{R}-2\frac{\rho'}{\rho}\frac{\mu'}{R}\right]X_3. \tag{22}$$

The boundary conditions in Eqs. (12) and (13) are written in terms of the new variables:

$$X_1(0)=X_3(0)=0, \tag{23}$$

$$X_1,X_3\to 0 \quad \text{as } y\to\infty. \tag{24}$$

2.2. Mean flow equations

The mean flow velocity and temperature profiles need to be calculated accurately for the solution of Eqs. (19)–(22). To this end, momentum equation:

$$2(\mu U')'+FU'=0, \tag{25}$$

and the energy equation:

$$2\left(\frac{\mu}{\sigma}T'\right)'+FT'=0, \tag{26}$$

have been solved. Here, $F'=\rho\mathrm{U}$, $T=T^*/T_e^*$ and $\sigma=\mu^*C_p^*/k^*$ is the Prandtl number. In the above, primes denote derivatives with respect to $y=y^*/L^*$ where $L^*=\sqrt{\frac{\nu_e^*x^*}{U_e^*}}$. Notice that Eq. (26) allows variable Prandtl numbers. Eqs. (25) and (26) are subject to the following boundary conditions:

$$F(0)=U(0)=0, \quad T(0)=T_w^*/T_e^*, \tag{27}$$

$$U,T\to 1 \quad \text{as } y\to\infty, \tag{28}$$

where T_w^* and T_e^* are the specified wall and freestream temperatures. Although the constant wall temperature case has been treated in this study, the constant heat flux case could also be treated easily. For the latter, Eq. (26) must be solved with the constant heat flux boundary condition and the stability problem is effected through the mean flow velocity and temperature profiles thus obtained.

In order to include the effects of variable properties in the analysis, the relevant parameters and their derivatives must be accurately calculated. Viscosity, density

and Prandtl number variations of water with respect to temperature are [6]:

$$\mu^* = 1.79369 * 10^{-3}/(35.155539 - 106.9718715T_r + 107.7720376T_r^2 - 40.5953074T_r^3 + 5.639148T_r^4), \quad (29)$$

$$\rho^* = 1002.28(0.803928 + 0.4615901T_r - 0.2869774T_r^2 + 0.0234689T_r^3), \quad (30)$$

$$\sigma = 13.66/(73.376906 - 208.7474538T_r + 197.7604676T_r^2 - 68.8626188T_r^3 + 7.4779458T_r^4), \quad (31)$$

where $T_r = T^*/273.16$, T^* is in Kelvin (K) and all quantities are in SI units. From this formulation, it can be seen that the kinematic viscosity of water, ν_{water}, decreases with increasing temperature.

On the other hand, Sutherland's viscosity law and the ideal gas relation have been used to determine the viscosity and the density of air, respectively:

$$\mu = \frac{\mu^*}{\mu_e^*} = \left(\frac{T^*}{T_e^*}\right)^{3/2} \frac{T_e^* + S_1^*}{T^* + S_1^*}, \quad (32)$$

$$\rho = \frac{\rho^*}{\rho_e^*} = \frac{T_e^*}{T^*}. \quad (33)$$

In Sutherland's law, S_1^* is a constant and for air $S_1^* = 110$ K [10]. For air, the Prandtl number has been taken to be a constant equal to 0.72 which is a good approximation for temperatures between −50 and 300 °C [10]. From the above relations, it can be seen that the kinematic viscosity of air, ν_{air} increases with increasing temperature.

Buoyancy effects may have been taken into account as well, however according to Schlichting [10], for the buoyancy forces to be of the same order of magnitude as the inertia and viscous forces, the Grashof number must be of the same order of magnitude as the Reynolds number squared, i.e. $G \approx R^2$, which occurs only when velocities are very low and temperature differences are very high. This has been checked for the lowest Reynolds number (critical Reynolds number R_{cr}) and the highest heating rate case both for air and water boundary-layer flows, and in each case the Grashof number turned out to be at least three orders of magnitude smaller than the Reynolds number squared. Therefore, buoyancy effects can be safely neglected for our purposes.

2.3. Transition prediction

For the transition calculations, the Smith–Van Ingen e^n method has been employed. As a wave travels in the flow direction, its angular frequency ω_r^* remains constant. The standard form of the dimensionless frequency is:

$$\Omega = \omega_r^* \nu^* / U_e^{*2} = \omega_r / R, \quad (34)$$

which also remains constant for a flat plate [12]. From Fig. 1, it can be seen that this wave at first passes through the stable region. It is damped until R_0, then amplified until R_1 and then damped again further downstream. At any station corresponding to $R > R_0$, amplitude A of a temporal normal mode having frequency Ω can be related to its amplitude A_0 at R_0 by using the following relation:

$$n = \ln\left(\frac{A}{A_0}\right) = 2\int_{R_0}^{R} \frac{\omega_i}{c_g} \mathrm{d}R. \quad (35)$$

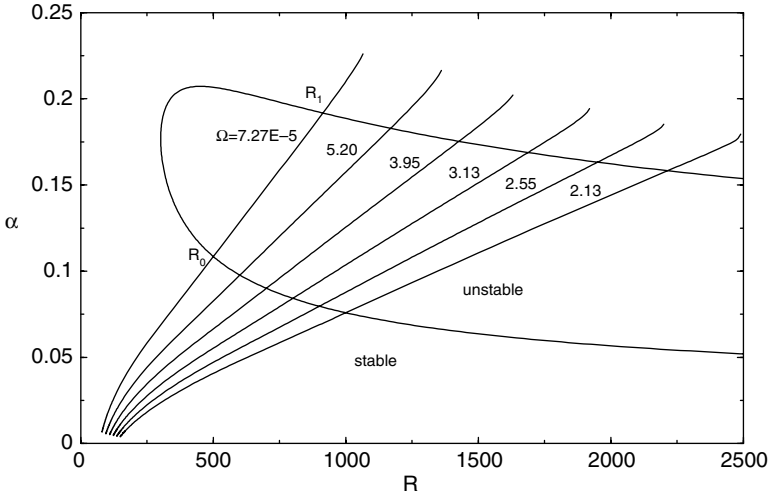

Fig. 1. Locations of points for several dimensionless frequencies for isothermal flow.

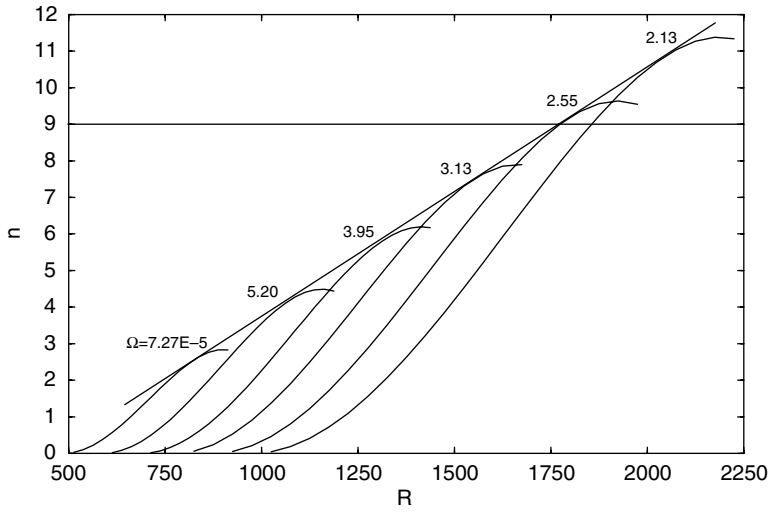

Fig. 2. Amplitude ratios for several dimensionless frequencies for isothermal flow.

In the above, $c_g = \partial\omega_r/\partial\alpha$ is the group velocity. The value of A_0 is linked to the disturbance environment through some receptivity mechanisms [13]. At each R, n represents the amplitude ratios of the disturbances.

Trajectories of constant frequency waves on a R–α graph are shown in Fig. 1 for the isothermal case. When the integral in Eq. (35) is evaluated for constant Ω values, the amplitude ratios depicted in Fig. 2 are obtained.

In Fig. 2, the curve that is tangent to all amplitude ratio curves is the envelope curve and determines the maximum amplification $e^{n_{max}}$ for a given Reynolds number. It has been found that the experimental transition data correlates well with $(A/A_0)_{max} \approx e^9$ as reported by Smith and Gamberoni [14]. Hence, according to these findings, $n_{max} = 9$ and this is the value used in this study.

It has to be pointed out that the linear stability theory can calculate neither A nor A_0, but it can calculate the total amplification as a normal mode travels through the unstable region which is sufficient for transition prediction using the e^n method.

3. Solution method

At a distance sufficiently far away from the wall, $U = 1$ and all y-derivatives are zero to a good approximation and Eqs. (19)–(22) have constant coefficients permitting solutions of the form:

$$\vec{X}^i = \vec{A}^i e^{\lambda_i y} \quad i = 1, 2, 3, 4. \tag{36}$$

Here, λ_i are the characteristic values, $\vec{X}^i$ and $\vec{A}^i$ are the four component solution and characteristic vectors corresponding to the ith characteristic value, respectively. Characteristic values of the above system are:

$$\lambda_{1,2} = \mp\alpha, \tag{37}$$

$$\lambda_{3,4} = \mp\left[\alpha^2 + iR(\alpha U - \omega)\right]^{1/2}. \tag{38}$$

Only the characteristic values with a negative sign are relevant because of the freestream conditions given in Eq. (24). Elements of the characteristic vectors corresponding to the remaining characteristic values can easily be found.

Elements of the characteristic vector corresponding to $\lambda_1 = -\alpha$:

$$a_1^1 = -i\alpha, \tag{39}$$

$$a_2^1 = i\alpha^2, \tag{40}$$

$$a_3^1 = 1, \tag{41}$$

$$a_4^1 = \frac{i}{\alpha}(\alpha U - \omega). \tag{42}$$

Elements of the characteristic vector corresponding to $\lambda_3 = -[\alpha^2 + iR(\alpha U - \omega)]^{1/2}$:

$$a_1^3 = 1, \tag{43}$$

$$a_2^3 = -\left[\alpha^2 + iR(\alpha U - \omega)\right]^{1/2}, \tag{44}$$

$$a_3^3 = i/\left[\alpha^2 + iR(\alpha U - \omega)\right]^{1/2}, \tag{45}$$

$$a_4^3 = 0. \tag{46}$$

The solution corresponding to λ_1 is the inviscid solution, whereas the solution corresponding to λ_3 is the viscous solution. With these, elements of the solution vector are as follows:

$$X_1(y) = -c_1 \mathrm{i}\alpha \mathrm{e}^{-\alpha y} + c_3 \mathrm{e}^{-\left[\alpha^2 + \mathrm{i}R(\alpha U - \omega)\right]^{1/2} y}, \tag{47}$$

$$X_2(y) = c_1 \mathrm{i}\alpha^2 \mathrm{e}^{-\alpha y} - c_3 \left[\alpha^2 + \mathrm{i}R(\alpha U - \omega)\right]^{1/2} \mathrm{e}^{-\left[\alpha^2 + \mathrm{i}R(\alpha U - \omega)\right]^{1/2} y}, \tag{48}$$

$$X_3(y) = c_1 \mathrm{e}^{-\alpha y} + c_3 \frac{\mathrm{i}}{\left[\alpha^2 + \mathrm{i}R(\alpha U - \omega)\right]^{1/2}} \times \mathrm{e}^{-\left[\alpha^2 + \mathrm{i}R(\alpha U - \omega)\right]^{1/2} y}, \tag{49}$$

$$X_4(y) = c_1 \frac{\mathrm{i}}{\alpha}(\alpha U - \omega)\mathrm{e}^{-\alpha y}, \tag{50}$$

where c_1 and c_3 are constants. These solutions provide the initial conditions for the integration of Eqs. (19)–(22). For the integration, a variable stepsize fourth order Runge-Kutta method has been used [15]. As integration proceeds from the freestream towards the wall, the viscous solution grows much faster than the inviscid solution and the linear independence between the two solutions is lost. Therefore, before this happens, Gram–Schmidt orthonormalization technique has to be used [8],[12]. For the current study, the algorithm has been applied at every $y = 0.1$ interval and no difficulties have been encountered.

The stability diagrams have been obtained using Newton iteration in two variables. This method requires two initial points on the curve so that the iteration can proceed in the specified Reynolds number direction. These two points have been found using a function minimization algorithm utilizing the simplex method [16]. At the nose region, Newton iteration fails and the procedure is repeated for the remaining branch of the curve so that the two branches meet at the nose region.

4. Results and discussion

The heat transfer effect manifests itself in two ways for the problem in hand. First, the velocity profile shape deviates from the Blasius profile due to variation of fluid properties with temperature. Second, additional terms having derivatives of viscosity and density appear in the stability equations. Viscosity varies in opposite trends with temperature for water and air so the effect of this parameter is expected to be different for these fluids. Therefore, stability and transition characteristics of water and air flows will be studied separately below.

4.1. Stability and transition characteristics of water flow

Dynamic viscosity of water decreases with increasing temperature and because of this a heated wall yields a negative second derivative of velocity at $y = 0$ (no inflection point in the profile) [6], see also Fig. 3b. Moreover, the velocity defects of the profiles become significantly less when the heat transfer rate is increased as can be seen from the profiles shown in Fig. 3a. This situation resembles the case of Falkner–Skan profiles with favorable pressure gradient.

Neutral stability curves for some heat transfer rates can be seen in Fig. 4. Apparently, heating the wall shifts the curves towards higher Reynolds numbers and hence

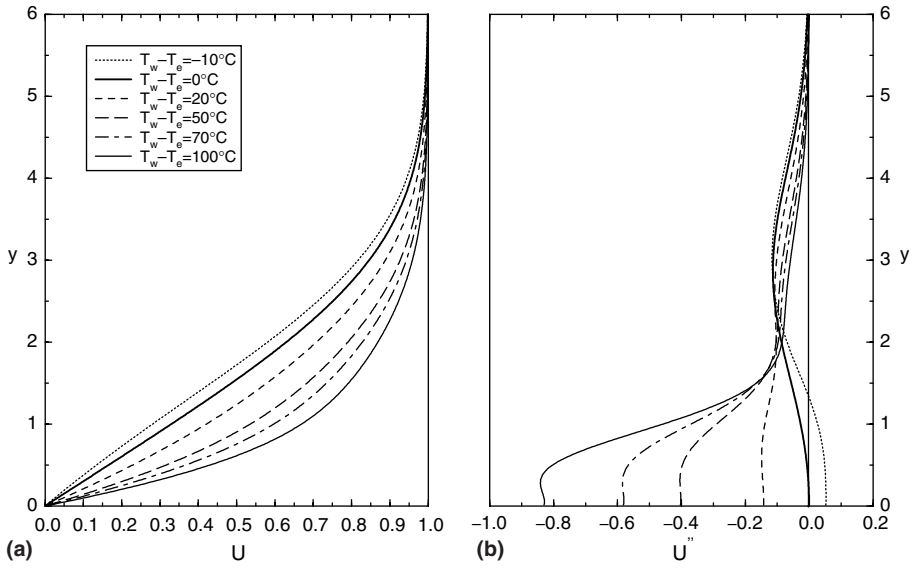

Fig. 3. (a) Velocity profiles and (b) profile curvature distributions in water for some heat transfer rates.

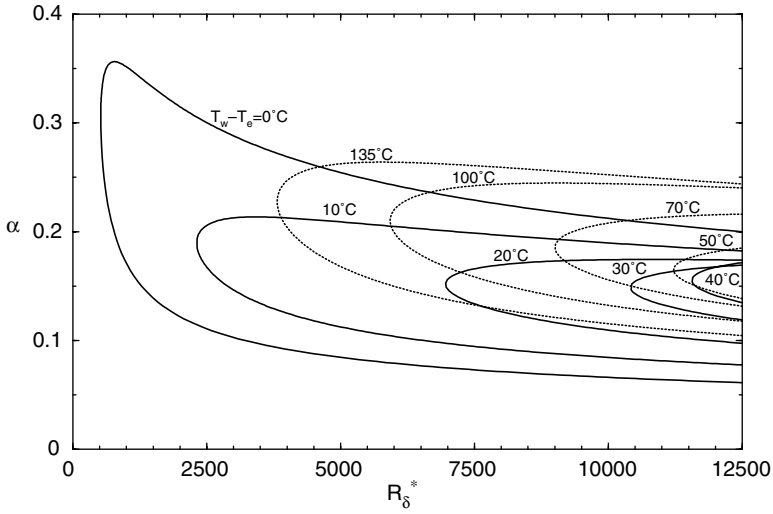

Fig. 4. Neutral stability curves for water flow with heated wall. Full lines depict cases where heating increases stability, whereas dotted lines show destabilizing heating.

has a stabilizing effect. There is a continuous and rapid increase in the critical Reynolds number until $T_w^* - T_e^* = 40$ °C case but as the wall is heated further, the stability curves start shifting towards lower Reynolds numbers. Therefore, there is an optimum wall temperature where the maximum stabilization is achieved. This reversed trend has been observed by Wazzan et al. [1] as well, almost at the same temperature observed here.

Neutral stability curves for cooled cases are depicted in Fig. 5. For the cooled cases, the critical Reynolds numbers are always smaller than the isothermal case. Furthermore, the neutral stability curve shapes are remarkably different from the heated and isothermal cases. At high Reynolds numbers, upper branches of the curves become flat which is typical of Rayleigh (or inviscid) instability. For these cases, the second derivative of the velocity profile vanishes at some distance from the wall and this implies instability according to Rayleigh's first theorem.

Having observed that heating has a stabilizing effect, one wonders what the dominant factor for this stabilization is. What differs in the heated case compared to the isothermal case is the velocity profile shape and the variable fluid properties. First of all, it is well known that

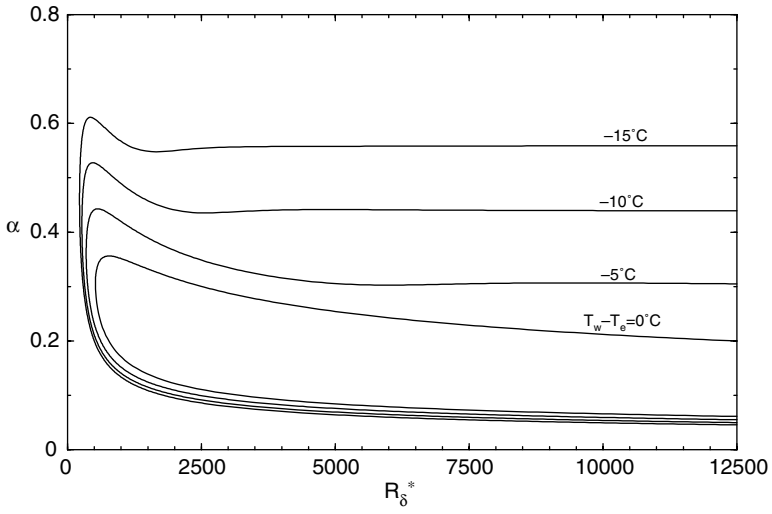

Fig. 5. Neutral stability curves for water flow with cooled wall.

profiles with smaller velocity defects are more stable as demonstrated by Falkner–Skan profiles. Therefore, the strong stabilization of heated water flows may be attributed to this factor. On the other hand, variable density and viscosity enter the problem through the stability equations as well and in order to get an idea about the individual and combined effects of these factors, a simple numerical experiment has been performed. For this, $T_w^* - T_e^* = 40$ °C case (the most stable case) has been selected. The results of this numerical experiment are summarized in Table 1. In the first four cases presented, the velocity profile obtained from non-isothermal equations of motion has been used. The first case in the table shows the result obtained by inserting the non-isothermal profile into the non-isothermal stability equations. The second case is for the non-isothermal profile fed into the isothermal stability equations. The third and fourth cases are again for the non-isothermal profile fed into the non-isothermal stability equations but with only the viscosity variation and the density variation allowed, respectively. The difference in the critical Reynolds numbers between the first and the second case suggests that the variable property terms in the stability equations have a strong destabilizing effect and this is mainly due to viscosity variation as can be inferred from the third and fourth cases. Here, it is more convenient to base the discussions on kinematic viscosity because it represents both the diffusivity (destabilizing effect) and dissipation (stabilizing effect). It appears that decreased kinematic viscosity near the wall (as a result of heating) destabilizes the flow.

Variable density has a very weak stabilizing effect, as can be seen from the same table. The effect is weak because water is essentially an incompressible fluid. Although the density is smaller near the wall and higher away from the wall (heavier fluid at the top), in the absence of gravitational effects this situation is stabilizing contrary to intuition because smaller fluid density near the wall increases the kinematic viscosity there and this is a stabilizing effect, in agreement with the discussion above.

For comparison, the critical Reynolds number corresponding to the isothermal Falkner–Skan profile with the same boundary-layer shape factor has also been included. The shape factor for the profile is 2.22 and the Falkner–Skan parameter is $\beta = 0.977$. The difference of the critical Reynolds numbers for this case and the second case is worth some attention because both of these results are coming from the isothermal stability equations for two different profiles having identical shape factors. This comparison shows that the boundary-layer shape factor alone is not sufficient to correlate stability data. The distribution of U and U' in the profile obviously plays a very important role. Moreover, a simple shape factor correlation cannot explain the destabilization occurring for heating rates greater than $T_w^* - T_e^* = 40$ °C.

Table 1
Critical Reynolds numbers given by isothermal and non-isothermal stability equation ($T_w^* - T_e^* = 40$ °C) (water)

Case	$R_{\delta^*\mathrm{cr}}$
$\mu = \mu(y)$, $\rho = \rho(y)$	11,562
$\mu = 1$, $\rho = 1$	21,413
$\mu = \mu(y)$, $\rho = 1$	11,501
$\mu = 1$, $\rho = \rho(y)$	21,433
$\mu = 1$, $\rho = 1$, $\beta = 0.977$	12,396

These results show that the main stabilizing effect is due to the velocity profile characteristics, whereas variable properties (in the stability equations) have a strong destabilizing effect. The latter effect can be reasoned physically as follows: as a result of heating, dynamic and kinematic viscosities of water increases as we move from the wall towards the freestream. It is well known that the kinematic viscosity has two roles in the stability phenomenon. First, it diffuses the vorticity created by high shear near the wall (destabilizing effect) and second, it dissipates the disturbance energy (stabilizing effect). At low Reynolds numbers the stabilizing effect is dominant but at high Reynolds numbers the destabilizing effect becomes important. The critical Reynolds number corresponds to the condition when these two effects are of equal strength. For heated cases, the critical Reynolds number increases because of the profile characteristics. On the other hand, due to the reduced kinematic viscosity near the wall, the disturbance energy created near the wall cannot be dissipated as effectively and therefore the disturbances are in a way trapped in to the thin shear layer near the wall. For this reason, kinematic viscosity stratification has a strong destabilizing effect but not strong enough to overcome the stabilizing effect of the velocity profile characteristics.

The critical Reynolds numbers obtained in the analysis have been compared to the results reported by other scientists in the literature. Fig. 6 depicts a comparison with the results reported by Wazzan et al. [1] for the entire range of heat transfer rates considered. It can be seen that the agreement is excellent for low to moderate heating rates but it is not as good for higher heat transfer rates. Our results are consistently lower than theirs. Surprisingly, the agreement gets better at highest heating rates. The maximum difference occurs at $T_w - T_e = 40$ °C where our result is 35% lower than theirs. The differences may be due to the way variable properties are treated in the two computations. For example, it is not clear whether variable Prandtl number effect has been taken into account by Wazzan et al. which may have a significant effect. Also, Wazzan et al. have solved a modified Orr–Sommerfeld equation that requires the second derivative of viscosity with respect to temperature. Keeping in mind that the viscosity law used is an empirical

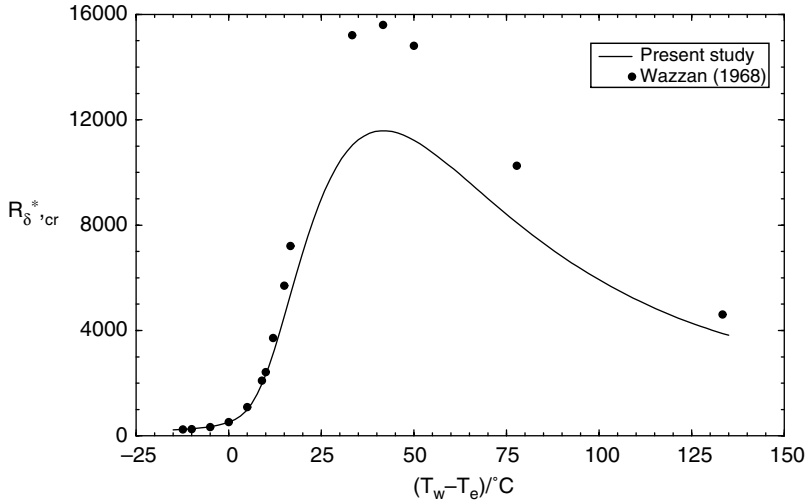

Fig. 6. Comparison of critical Reynolds numbers calculated by Wazzan et al. and the present study for water flow.

one, higher order derivatives will normally amplify the errors introduced with this law. Therefore, the present formulation has an advantage over the one used by Wazzan et al. in the sense that it requires only the first derivative. On the other hand, Wazzan et al. mention that the critical Reynolds number for the non-isothermal profile using the isothermal Orr–Sommerfeld equation is 140,000 which seems to be an order of magnitude higher than the results found in the present study. Although the shape factor is not a good parameter to correlate stability data for the current problem, it is hard to understand why such a high critical Reynolds number has been obtained while the Falkner–Skan profile with a similar shape factor yields a much smaller critical Reynolds number. With no heat transfer related terms, the Orr–Sommerfeld equation has only the velocity and second derivative of velocity to work with and two profiles should yield critical Reynolds numbers at least with comparable magnitudes.

In spite of all this, the trends of the critical Reynolds numbers have been well captured by both calculations and the temperature where the stability reversal occurs is in remarkable agreement. As a result, the agreement is judged to be fair.

The studies on the current topic reported in the literature are based on various methods like asymptotic, perturbation, shooting and finite difference methods. Examples to perturbation and asymptotic studies are those of Hauptmann [2] and Herwig and Schäfer [3], respectively and are valid for small heating rates. The method used by Wazzan et al. [1] is a shooting method like the present study. On the other hand, Lee [5] has used a finite difference method. A separate graph for comparisons with the results of the aforementioned studies is presented in Fig. 7. While the agreement is excellent for all data sets for low heating and cooling rates, deviations become larger with increasing heat transfer rates. Maximum deviations typically occur at the highest value of the heat transfer rate depicted in the figure. Overall agreement is very good but the present results agree best with those of Lee. Asymptotic and perturbation results deviate from the general trend outlined by higher order methods as the heat transfer rate increases, as expected.

The results of the transition calculations are presented in Fig. 8. Also included in the figure are the numerical results of Lee [5]. The trend for the variation of the transition Reynolds numbers with increasing heating rate is similar to that observed in critical Reynolds numbers. The transition Reynolds number increases as heating rate increases until $T_w^* - T_e^* = 45°$, but starts decreasing beyond this value of the heating rate. The mechanisms causing this trend reversal are similar to those causing it for critical Reynolds numbers. Trend reversal is observed almost at the same temperature as in the critical Reynolds number case. Although early loss of stability (low critical Reynolds number) generally implies early transition, it is usually not possible to predict the transition Reynolds number as a function of the critical Reynolds number alone. In addition to the critical conditions, an important parameter here is the total amplification as a function of the wave frequency. This functional relationship can only be established through a thorough stability analysis using a method like the one outlined in Section 2.3, and each case must be treated separately.

On the other hand, the comparison of the present results with those reported by Lee [5] show very close agreement. The results given by Lee are for low heat transfer rates so whether the trend reversal occurring

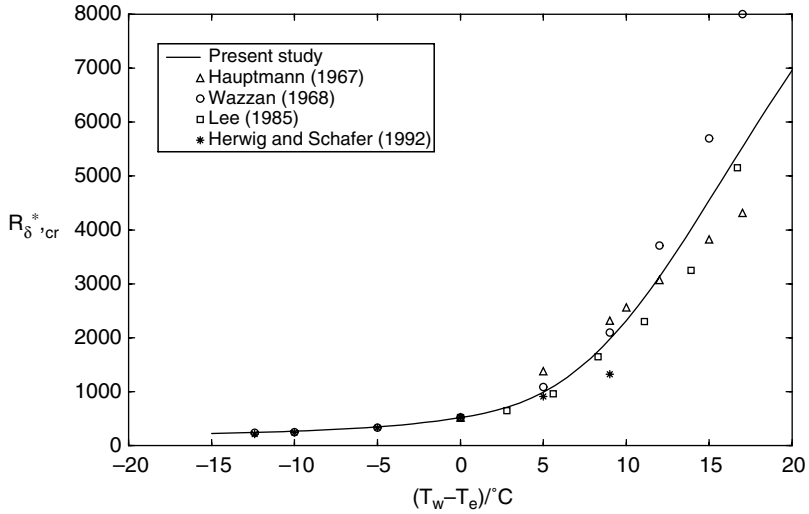

Fig. 7. Comparison of critical Reynolds numbers reported in the literature with those of the present study for water flow with low heat transfer rates.

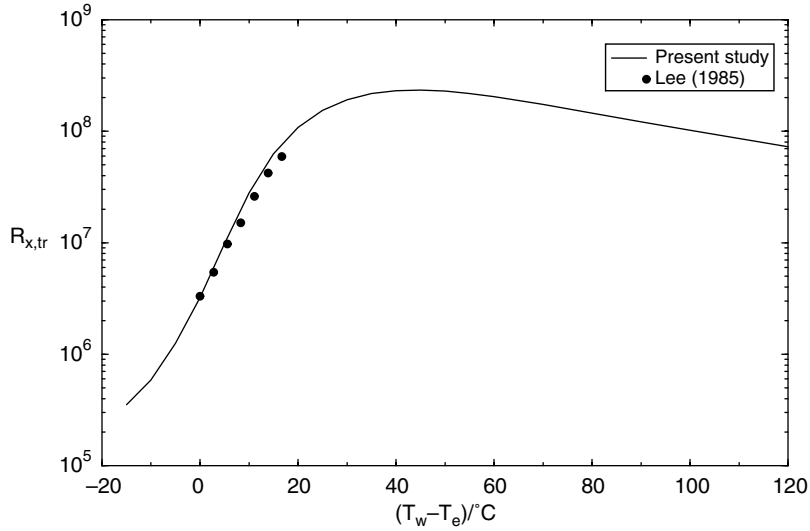

Fig. 8. Comparison of transition Reynolds numbers calculated by Lee and the present study for water flow.

at higher heating rates is observed in that study or not is unknown. It should be noted that Lee has used a modified Orr–Sommerfeld equation in his study and his results have been extracted from the graphs given in Ref. [6] so part of the already small discrepancy can be attributed to that.

4.2. Stability and transition characteristics of air flow

Dynamic and kinematic viscosity increases with increasing temperature for air which is an opposite trend compared to that of water so one would expect the stability characteristics of heated air flow to be different from those of water. First of all, an inflection point occurs in the boundary-layer profile (see Fig. 9b) which immediately calls for Rayleigh instability. Therefore, at this point, it is appropriate to look at the effect of heating on the profile shapes, which are shown in Fig. 9a.

As can be seen, heating increases the velocity defect in the profiles which usually means reduced stability. On the other hand, the effect of heating is less pronounced for air flow than for water flow. This is due

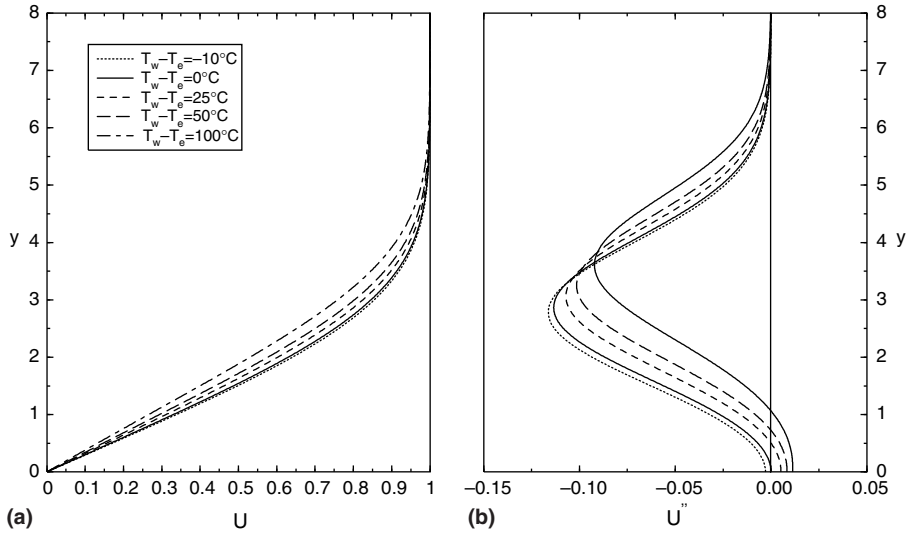

Fig. 9. (a) Velocity profiles and (b) profile curvatures in air for some heat transfer rates.

to the fact that temperature dependence of viscosity is much stronger for water than it is for air.

Fig. 10 depicts the neutral stability curves computed for heated air flow. Contrary to water, air flow is continuously destabilized with increasing heat transfer rate. However, the destabilization is not as strong as the stabilization of water. This is again due to relatively weak dependence of viscosity on temperature for air. Moreover, there is no reversal of stability characteristics at a critical heating rate. Although heating increases the kinematic viscosity near the wall (stabilizing effect) besides increasing the velocity defect (destabilizing effect), this is not enough to stabilize the flow even at low Reynolds numbers where the stabilizing effect of kinematic viscosity is most dominant.

Variation of the critical Reynolds number with heat transfer rate is illustrated in Fig. 11. Also included are the results reported by Hauptmann [2] and Schäfer et al. [4]. These results are for low heat transfer rates and it can be seen that the agreement is very good, especially with Hauptmann. As mentioned before, the results reported by other scientists in the literature are mostly from asymptotic or perturbation methods valid for low heating rates. The deviation of these results from the results of the present study is mainly due to this. It is surprising that the results of Hauptmann, although

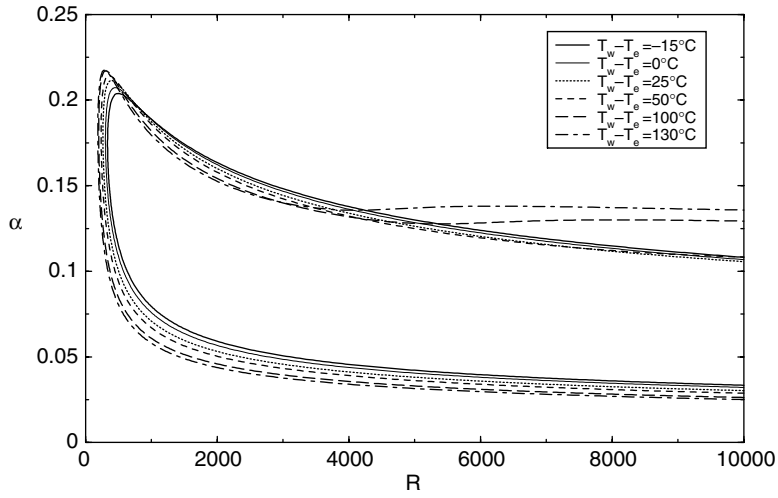

Fig. 10. Neutral stability curves for air flow with heated wall.

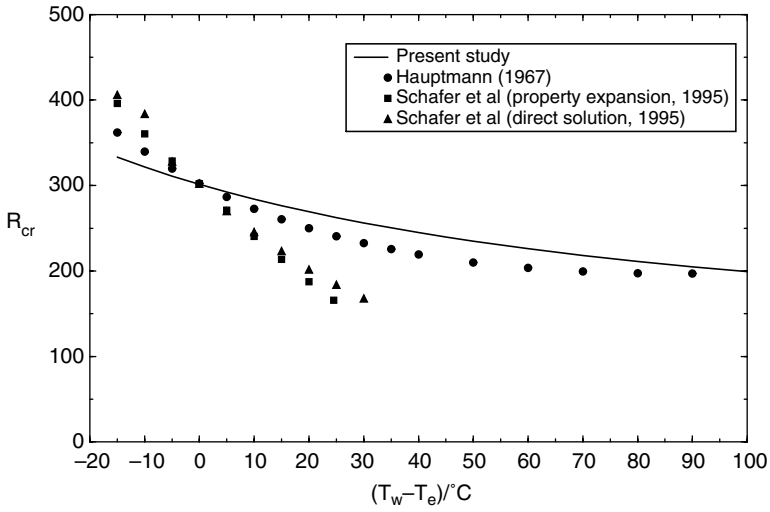

Fig. 11. Comparison of critical Reynolds numbers calculated by Hauptmann, Schäfer et al. and the present study for air flow.

obtained from an older and simpler analysis keep up very well with the results of the present study for the entire range of heat transfer rates considered here.

The results of the present study have also been compared with the experimental data of Harrison et al. [17] and the results are shown in Fig. 12. Here the parameter $\epsilon = (T^*_w - T^*_e)/T^*_e$. Although there is some scatter in the experimental data, in overall the results are in good agreement and the decreasing trend has been well captured by the computations. The current results are systematically higher than the experimental ones, the deviation increasing with increasing heat transfer rate.

A similar check to that made for water flows has also been made here in order to assess the individual and combined effects of the factors involved in the problem and the results are presented in Table 2. Again, the first four cases are for the non-isothermal velocity profile inserted into various forms of the stability equations modified for individual or combined effects of variable viscosity and density. The fifth case corresponds to an isothermal profile with the same boundary-layer shape factor as the non-isothermal profile fed into the isothermal stability equations. From the first and second cases, we understand that the combined effect of variable viscosity and density terms in the stability equations is stabilizing. On the other hand, the results of the second and third cases show that variable viscosity terms alone are stabilizing just like variable density terms alone as could

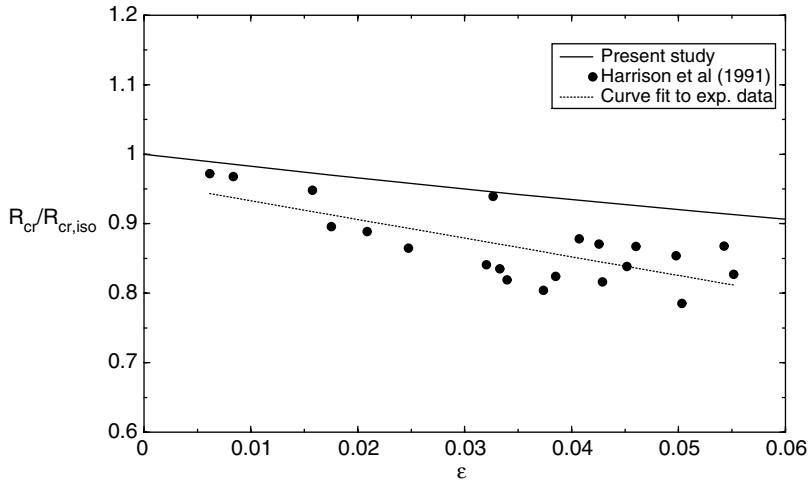

Fig. 12. Comparison of critical Reynolds numbers of the present study with the experimental data of Harrison et al. for air flow.

Table 2
Critical Reynolds numbers given by isothermal and non-isothermal stability equation ($T_w^* - T_e^* = 130$ °C) (air)

Case	R_{cr}
$\mu=\mu(y)$, $\rho=\rho(y)$	185.05
$\mu=1$, $\rho=1$	119.50
$\mu=\mu(y)$, $\rho=1$	145.90
$\mu=1$, $\rho=\rho(y)$	152.78
$\mu=1$, $\rho=1$, $\beta=-0.1922$	23.63

be inferred from the results of the second and the fourth cases. It is noteworthy that variable density has a more significant effect for air flows than it has for water flows. Although there is an adverse density stratification here, the gravitational effects have not been taken into account and the only role of density here is to increase the kinematic viscosity near the wall and this enhances the stabilizing effect of the latter parameter. This trend is in agreement with the case of water flow, where adverse density stratification (in the absence of gravity) causes stabilization as well.

Comparing the results of the second and fifth cases, we again understand that the boundary-layer shape factor alone is not sufficient to correlate stability data. Although the same isothermal equations have been used for the two profiles, we see that the non-isothermal profile is significantly more stable.

On the other hand, the transition calculations reveal that the variation of the transition Reynolds number resembles that of critical Reynolds numbers very closely, i.e. there is a monotonous decrease with increasing heat transfer rate as depicted in Fig. 13. As can be expected, the variation is not very strong again because of weak dependence of air viscosity on temperature. Here, we see once more that the critical conditions are closely related to transition conditions.

Fig. 14 shows the comparison of present results with experimental data given by Liepmann and Fila [7]. Liepmann and Fila have conducted their experiments in a low-turbulence wind tunnel and have reported two sets of data, one corresponding to a turbulence level of $T_u=0.0005$ and the other to $T_u=0.0017$. For the comparisons, the e^n method has been employed with a value of n given by the following empirical formula which is valid for $T_u>0.001$ [6]:

$$n = -8.43 - 2.4 \ln T_u. \tag{51}$$

Accordingly, for $T_u=0.0017$, $n=6.875$. $T_u=0.0005$ is outside the range of validity of the above formula so $n=9$ has been retained for that data set. On the other hand, it is not clear whether this formula can be used for flows with heat transfer. However, we understand from Ref. [13] that $n=9$ can be used even for compressible flows with heat transfer, so using the above formula for low speed flows such as the ones treated in this study should not cause any problems.

Although the decreasing trend with increasing heat transfer rate has been well captured both by the experimental data and the numerical results, there are severe differences between the numerical values for the transition Reynolds numbers. The predictions of the present method is approximately five to six times greater than the experimental values. There can be several reasons for this discrepancy, the most likely one being the way transition is defined in both studies. Liepmann and Fila clearly mention in their report that the first appearance of turbulent bursts—that is occasional sudden changes from a laminar profile to a turbulent profile—is taken as the transition location. However, e^n method predicts

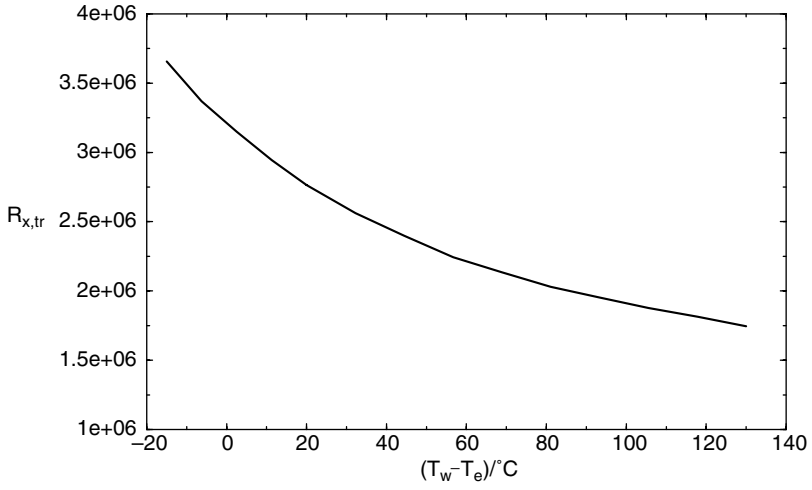

Fig. 13. Variation of the transition Reynolds number with heat transfer rate for air flow.

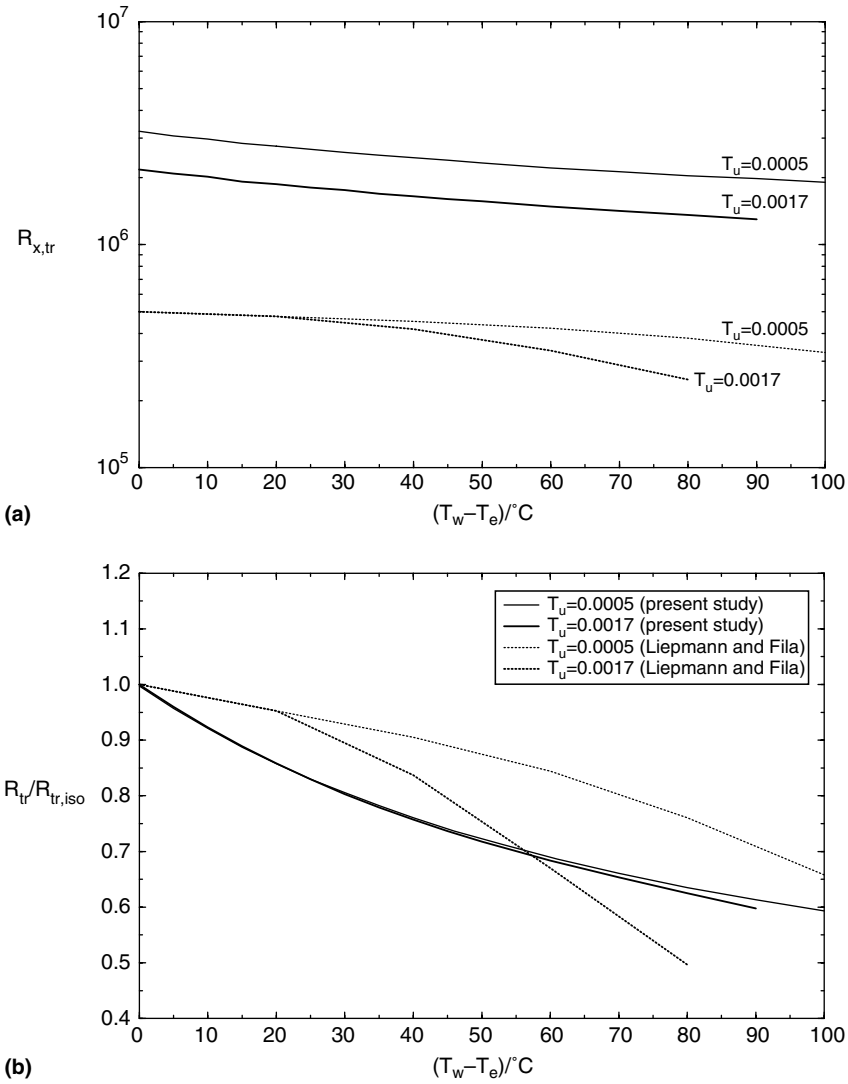

Fig. 14. Comparison of experimental transition Reynolds numbers obtained by Liepmann and Fila (dotted curves) with the results of and the present study (full curves) for air flow.

breakdown to turbulence location which is a later stage of the transition process [10]. Therefore, it is reasonable that the computed transition Reynolds numbers are much higher than the experimental ones. Other factors that may be contributing to the discrepancy are non-parallel effects and buoyancy which have not taken into account in the present study. Liepmann and Fila mention that the freestream velocity was 8.19 m/s during the experiments which can make non-parallelism an important factor. For isothermal flows, critical Reynolds numbers calculated by solving the Orr–Sommerfeld equation and those observed during experiments have been compared in the past by different investigators and the experimental results were found to be typically 20–25% lower [18]. It can be argued that the transition Reynolds numbers calculated and measured could also be similarly discrepant for isothermal flows. This suggests that, non-parallelism could be an important factor even for isothermal flows. Therefore, at least part of the difference between the numerical results reported in this study and the experimental results reported by other scientists is due to non-parallelism.

When each set of data in Fig. 14a is normalized by its respective isothermal transition Reynolds number, part of the discrepancy is removed as can be seen from Fig. 14b. Although experimental and numerical data still do not agree well, it has to be remembered that the experimental data of Liepmann and Fila have considerable

scatter. When this and other considerations mentioned above are kept in mind, the agreement is decidedly fair.

Although not specified in the report of Liepmann and Fila, surface roughness may be another factor contributing to the disagreement of the results.

Another point worth mentioning is that for low heat transfer rates, the experimental transition Reynolds numbers for $T_u = 0.0005$ and $T_u = 0.0017$ are identical which is not reflected by the results of the present study.

The decreasing trend of the transition Reynolds number with increasing heat transfer rate has also been observed and reported by Higgins and Pappas [19] although the flow there is supersonic at a Mach number of 2.4.

5. Conclusions

Stability and transition characteristics of heated water and air flows have been studied numerically using the linear stability theory. The results obtained show that these characteristics are quite different for the two fluids considered. Generally speaking, heating stabilizes water flows, whereas it destabilizes air flows. It has been shown that the boundary-layer velocity profile has the strongest effect on the stability and transition characteristics. The variable viscosity terms in the stability equations also have a strong effect for both of the fluids considered. Finally, density has a significant effect on air flows but its effect on water flows is negligible. When the effects of variable viscosity and density in the stability equations are combined so that the discussion is based on the kinematic viscosity only, it has been inferred that decreasing kinematic viscosity near the wall has a destabilizing effect.

The method used in this study is quite general in the sense that it can be extended to treat flows with different geometries and regimes with varying levels of modifications and extensions. For example, three dimensional mean flows could be treated with two or three dimensional disturbances. Axisymmetric flows and flows with pressure gradient can also be treated after a modest effort for the modification of the governing equations. The method can also be used for studying supersonic and even hypersonic flows. For the problem in hand, the method is not limited to low heat transfer rates for heated flows. These are advantages over most of the other methods used to solve the similar problem as those methods are either limited to low heat transfer rates or are not fit for extension to treat different geometries and flow regimes.

References

[1] A.R. Wazzan, T. Okamura, A.M.O. Smith, The stability of water flow over heated and cooled flat plates, J. Heat Mass Transfer 90 (1968) 109–114.
[2] E.G. Hauptmann, The influence of temperature dependent viscosity on laminar boundary-layer stability, Int. J. Heat Mass Transfer 11 (1967) 1049–1052.
[3] H. Herwig, P. Schäfer, Influence of variable properties on the stability of two-dimensional boundary layers, J. Fluid Mech. 243 (1992) 1–14.
[4] P. Schäfer, J. Severin, H. Herwig, The effect of heat transfer on the stability of laminar boundary-layers, Int. J. Heat Mass Transfer 38 (1995) 1855–1863.
[5] D.Q. Lee, Stability and Transition Characteristics of Water Boundary-Layers with Heat Transfer, MSc Thesis, California State University, Long Beach, CA, 1985.
[6] T. Cebeci, J. Cousteix, Modeling and Computation of Boundary-Layer Flows, Horizons Publishing Inc., Long Beach, 1999, pp. 179–190.
[7] H.W. Liepmann, G.H. Fila, Investigations of effects of surface temperature and single roughness elements on boundary-layer transition, NACA Report No. 890, 1947.
[8] L.M. Mack, Boundary layer stability theory, AGARD Report No. 709, 1984.
[9] S. Özgen, G. Degrez, G.S.R. Sarma, Two-fluid boundary-layer stability, Phys. Fluids 11 (1998) 2746–2757.
[10] H. Schlichting, Boundary-Layer Theory, McGraw-Hill, New York, 1979.
[11] C.-S. Yih, Stability of two-dimensional parallel flows for three-dimensional disturbances, Q. Appl. Math. 12 (1954) 434–435.
[12] L.M. Mack, A numerical study of the temporal eigenvalue spectrum of the Blasius boundary-layer, J. Fluid Mech. 73 (1976) 497–520.
[13] D. Arnal, Progress in transition modelling, AGARD Report No. 793, 1994.
[14] A.M.O. Smith, N. Gamberoni, Transition, pressure gradient and stability theory, Douglas Aircraft Co. Rept. ES 26388, 1956.
[15] J.H. Mathews, Numerical Methods, Prentice-Hall, London, 1987, pp. 423–432.
[16] W.H. Press, S.A. Teukolsky, W.T. Vetterling, B.P. Flannery, Numerical Recipes in Fortran 77, Cambridge University Press, Cambridge, 1992, pp. 402–406.
[17] S.B. Harrison, D.J. Mee, T.V. Jones, Experiment on the influence of heating on boundary-layer transition in favourable pressure gradients, in: Proceedings Eurotherm Seminar No. 25, Pau, France, 1991.
[18] S.J. Cowley, X. Wu, Asymptotic approaches to transition modelling, AGARD Report No. 793, 1994.
[19] R.W. Higgins, C.C. Pappas, An experimental investigation of the effect of surface heating on boundary-layer transition on a flat plate in supersonic flow, NACA TN 2351, 1951.